ARTICLE

Assembly and Functionalization of DNA–Polymer Microcapsules

Francesca Cavalieri,[†,‡] Almar Postma,[†] Lillian Lee,[†] and Frank Caruso[†,*]

[†]Centre for Nanoscience and Nanotechnology, Department of Chemical and Biomolecular Engineering, The University of Melbourne, Parkville, Victoria 3010, Australia, and [‡]Dipartimento di Scienze e Tecnologie Chimiche, Università di Roma Tor Vergata, 00173 Roma, Italy

ABSTRACT We report the synthesis and characterization of DNA-grafted poly(*N*-isopropylacrylamide) (PNIPAM) micelles, their assembly into multilayered thin films, and the subsequent generation and poly(ethylene glycol) (PEG) functionalization of DNA–PNIPAM microcapsules. Multilayer films were assembled by sequentially depositing DNA-grafted PNIPAM micelles containing the cDNA sequences polyA$_{30}$ or polyT$_{30}$ (*i.e.*, PNIPAM-A$_{30}$ or PNIPAM-T$_{30}$). DNA–polymer microcapsules were obtained by the alternate deposition of PNIPAM-A$_{30}$ and PNIPAM-T$_{30}$ onto silica particles, followed by removal of the template core. Upon removal of the silica core particle, shrinkage of between 30 and 50% was observed for the microcapsules. The presence of PNIPAM within the DNA–polymer hybrid film reduces the permeability of the microcapsules to macrosolutes (*e.g.*, dextran) compared with microcapsules made solely of DNA. The hydrophobic core of the DNA-grafted PNIPAM micelles was designed to contain alkyne "click" groups, which were exploited to covalently couple azide-bearing low-fouling PEG to the DNA–PNIPAM microcapsules. The combination of hydrophobic and reactive "click" nanodomains, along with the degradability of DNA, offers a multifunctional and versatile DNA–polymer capsule system that is envisioned to find applications in the controlled delivery of therapeutics.

KEYWORDS: microcapsules · oligonucleotides · DNA · self-assembly · micelles · layer-by-layer

The assembly of DNA–polymer conjugates into complex architectures has led to functional materials for use in DNA detection,[1–3] DNA-templated synthesis,[4] and DNA purification.[5,6] Amphiphilic DNA block copolymers[7,8] constitute an important class of building blocks for the assembly of DNA–polymer materials. In aqueous solution, such copolymers readily self-assemble into spherical micelles with a hydrophobic polymeric core and single-stranded (ss) oligonucleotides as the surrounding hydrophilic corona. A recent example deals with micellar aggregates of DNA-poly(propyleneoxide) block copolymers (DNA-*b*-PPO), which exhibit shape versatility, altering from spherical to rodlike aggregates upon hybridization.[9,10] These ordered structures have also been used as substrates for DNA polymerase to tune the nanoparticle size[11] and as a platform for chemotherapeutic drug delivery.[12,13] Advances in the application of DNA–polymer materials in, for example, therapeutics and diagnostics, rely on the rational design and controlled assembly of such conjugates into higher order nano- and micrometer-scale materials. Additionally, nanoengineered functional DNA–polymer materials can exploit both the recognition properties of DNA and the responsiveness of the polymer to tailor the structural and physicochemical properties of such systems.

Herein, we report the synthesis of DNA-grafted polymer micelles (Scheme 1a) and their assembly into multilayered thin films and microcapsules (Scheme 1b). The synthesized oligonucleotide-grafted poly(*N*-isopropylacrylamide) (PNIPAM) micelles, bearing cDNA sequences (PNIPAM-A$_{30}$ and PNIPAM-T$_{30}$), were layer-by-layer (LbL) assembled into stable films/capsules by exploiting hybridization between the oligonucleotides. We demonstrate that the DNA–polymer microcapsules are considerably less permeable than single-component DNA capsules. Further, we show that the capsules can also be modified by functionalization with low-fouling poly(ethylene glycol) (PEG). We sought to explore this approach to develop a platform for the engineering of multifunctional DNA–polymer colloidal carrier systems, and also to improve the stability and modify the permeability properties of single-component DNA microcapsules obtained by the LbL assembly of diblock oligonucleotides.[14–16] In this paper, we focus on the synthesis of the DNA–polymer building blocks, their assembly into functional films and capsules, examination of the physicochemical properties (permeabil-

*Address correspondence to fcaruso@unimelb.edu.au.

Received for review October 22, 2008 and accepted December 05, 2008.

Published online January 9, 2009.
10.1021/nn800705m CCC: $40.75

ity) of the capsules, and their functionalization. The DNA−polymer capsules reported are ultimately expected to have potential for the controlled delivery of therapeutics, as the materials incorporate the benefits of nanoscale polymeric micelles (for loading lipophilic drugs),[17] a high-volume capsule interior (for loading macromolecules such as DNA, peptides, and proteins),[18] and degradability, which can be triggered by the presence of DNase.[19]

RESULTS AND DISCUSSION

Preparation and Characterization of PNIPAM-A_{30} and PNIPAM-T_{30} Micelles. We first synthesized a novel and versatile random terpolymer, PNIPAM-*co*-PA-*co*-NAS, comprising poly(*N*-isopropylacrylamide) (PNIPAM), bearing hydrophobic propargyl ester groups and *N*-hydroxysuccinimide (NHS) reactive moieties. The hydrophobically modified PNIPAM-*co*-PA-*co*-NAS (16 000 g mol^{-1}) was prepared by reversible addition−fragmentation chain transfer (RAFT) polymerization (see Figure S1 for the polymer structure). Controlled radical copolymerization *via* RAFT was chosen because of its monomer compatibility, good end-group purity, and control over the chain composition and architecture.[20,21] This allowed us to design and synthesize a terpolymer with a homogeneous composition of reactive monomers. The PNIPAM terpolymer was found to form micelle-like nanoparticles below its lower critical solution temperature (LCST = 29 °C). We specifically designed the terpolymer so that upon assembly the hydrophobic core would contain alkyne "click" groups that could then be used to covalently couple azide-bearing species to the micelles via the copper(I)-catalyzed Huisgen 1,3-dipolar cycloaddition reaction.[22] Attractive features of this reaction include its high efficiency, selectivity, and ability to proceed under mild reaction conditions.[22] Furthermore, the functional hydrophobic interior also permits the micelles to be loaded with lipophilic drugs. The presence of 5% hydrophobic propargyl ester pendant groups (stickers) on the hydrophilic PNIPAM chain was found to trigger both intra- and interchain associations with water, forming flowerlike micelles. The stickers condense in the center and the hydrophilic segments between the stickers are excluded to the outside, forming flowerlike petals (Scheme 1a). Similar assembly behavior has been observed for other polymers[23] and telechelic PNIPAM with octadecyl chain ends.[24]

The formation of hydrophobic domains was investigated using pyrene as a fluorescent probe in combination with dynamic light scattering (DLS) measurements (Figure 1). Both studies indicated that below the solution "cloud point", the PNIPAM terpolymer exists as flowerlike micellar aggregates in solution. A strong enhancement in pyrene fluorescence was observed with increasing PNIPAM terpolymer concentration in aqueous solution (Supporting Information, Figure S2). This indicates the transfer of pyrene from water to the hydrophobic domain of the polymer micelle-like nanoparticles. The critical aggregation concentration (cac) was determined to be 0.08 mg mL^{-1}. This was obtained by taking the crossover value of the intensity ratio be-

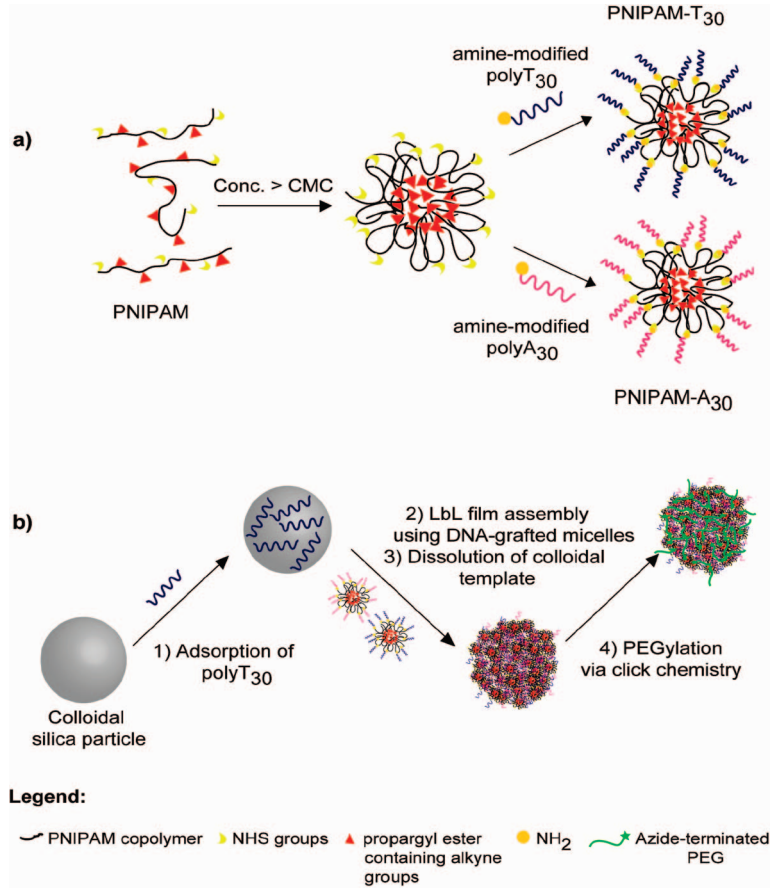

Scheme 1. Schematic representation of (a) formation of PNIPAM-A_{30} and PNIPAM-T_{30} micelles, and (b) multilayer assembly of PNIPAM-A_{30} and PNIPAM-T_{30} micelles onto particles, removal of the template particle, and functionalization via "click" chemistry to afford PEGylated DNA−PNIPAM capsules.

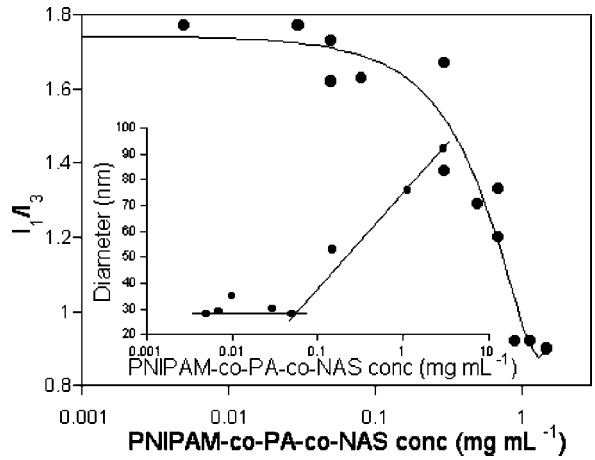

Figure 1. I_1/I_3 emission ratio and diameter (inset) as a function of the PNIPAM random terpolymer concentration.

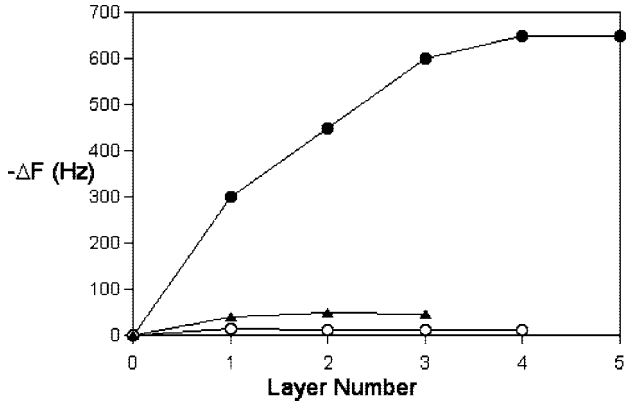

Figure 2. QCM data comparing the assembly of five PNIPAM-A_{30}/PNIPAM-T_{30} layers (●), three layers of PNIPAM micelles (▲), and four layers of the homopolymeric blocks of polyA_{30}/polyT_{30} (○). Layer 0 corresponds to polyT_{30}.

tween the first (I_1) and the third (I_3) emission peaks, I_1:I_3, as a function of the hydrophobized polymer concentration (Figure 1). The hydrodynamic radius (R_h) of the PNIPAM random terpolymer in aqueous solution, determined by dynamic light scattering (DLS), remained constant at 15 ± 5 nm until the concentration reached the cac of 0.05−0.08 mg mL^{-1} (Figure 1, inset). A further increase in the polymer concentration (to *ca.* 3 mg mL^{-1}) resulted in a significant increase in R_h up to 45 ± 15 nm. Active NHS groups located on the hydrophilic micelle corona were then coupled directly with the 5′-end amine-modified oligonucleotides polyT_{30} or polyA_{30}, providing building blocks with unique sequence-specific recognition properties. PNIPAM-A_{30} and PNIPAM-T_{30}, in 0.5 M NaCl, were found to have a diameter of 40 ± 15 nm by DLS (Figure S3).

Multilayer Assembly of PNIPAM-A_{30} and PNIPAM-T_{30} Micelles. The LbL assembly of PNIPAM-A_{30} and PNIPAM-T_{30} micelles, and of the corresponding oligonucleotides A_{30}/T_{30}, was followed using a quartz crystal microbalance (QCM). A polyT_{30} precursor layer was first adsorbed on the surface followed by a layer of polyA_{30}. When polyT_{30} was introduced after the second layer, limited hybridization was observed owing to competitive hybridization of polyT_{30} to double-stranded polyT_{30}/polyA_{30} present on the surface (Figure 2). In contrast, a considerable decrease in QCM frequency (corresponding to an increase in adsorbed mass of the micelles) was observed for the consecutive adsorption of PNIPAM-A_{30} and PNIPAM-T_{30} layers (up to four layers), after which a plateau in QCM frequency was observed. Both PNIPAM-A_{30} and PNIPAM-T_{30} micelles act as multifunctional building blocks and result in DNA strands being available for hybridization in subsequent layers. The progressive decrease in the magnitude of the change in QCM frequency with increasing layer number is ascribed to the enhanced steric hindrance resulting from the adsorbed micelles within the composite multilayer. The frequency changes observed for deposition of PNIPAM-A_{30} and PNIPAM-T_{30} in the first three layers (>150 Hz/layer) are significantly larger than those observed for multilayer films assembled by hybridization of diblock oligonucleotides (20−60 Hz/layer).[14−16] Adsorption of PNIPAM-A_{30} and PNIPAM-T_{30} occurred over 2 h, suggesting a complex deposition mechanism with possible film rearrangement occurring upon adsorption of each micelle layer. To facilitate buildup of the multilayer films, a high ionic strength (0.5 M NaCl, SSC buffer) solution was used. The high salt concentration reduces the repulsive electrostatic interactions between DNA strands. Adsorption of the DNA−PNIPAM micelles on the surface is mainly driven by complementary oligonucleotide hybridization, as unmodified PNIPAM micelle adsorption of several layers was found to be limited to a frequency shift of approximately 50 Hz (Figure 2).

DNA−PNIPAM Microcapsule Formation. The assembly of five layers of PNIPAM-A_{30} and PNIPAM-T_{30} was also conducted on 3- and 6-μm diameter silica particles. To confirm hybridization of complementary oligonucleotides, the PNIPAM-A_{30}/PNIPAM-T_{30}-coated particles were incubated with PicoGreen, a DNA double-strand specific dye.[25] The denaturation of the double-stranded DNA present in the PNIPAM-A_{30} and PNIPAM-T_{30} multilayer film on the particles was profiled by monitoring the fluorescence intensity of PicoGreen to assess whether the presence of double-stranded oligonucleotides stabilizes the multilayered thin film (Figure S4). An intense fluorescent ring was observed on both the core−shell particles (Figure 3a) and microcapsules (Figure 4b), indicating that hybridization of the PNIPAM-A_{30} and PNIPAM-T_{30} micelles results in the formation of a stable film with a melting temperature of 62 °C (Figure S4). However, the large frequency change (Figure 2) and the slow deposition kinetics (2 h) observed by QCM suggest that in addition to hybridization, a secondary slower process is present in the buildup of the multilayer films.

The high local polymer concentration and ionic strength experienced by the micelles within the layer structure are favorable conditions for the self-aggregation and collapse of the PNIPAM flowerlike micelles on the surface. Salt-induced dehydration and collapse of a PNIPAM layer on silica substrates into tighter polymer coils is well-known.[26,27] The large deposition of mass in the first layers (see Figure 2) and the collapse of micelles upon surface adsorption may therefore bury the oligonucleotides, sterically hindering further hybridization and thus limiting the deposition of the subsequent layers. To corroborate this hypothesis, PNIPAM-A_{30}/PNIPAM-T_{30}-coated particles were incubated with rhodamine-labeled PNIPAM micelles after the deposition of five alternating layers of PNIPAM-A_{30} and PNIPAM-T_{30}. The incorporation of the fluorescently labeled PNIPAM micelles into the multilayers reflects the interaction of the micelles with the polymer domains within the multilayers (Figure 3c). As PNIPAM micelles are known at high concentration to interact through hy-

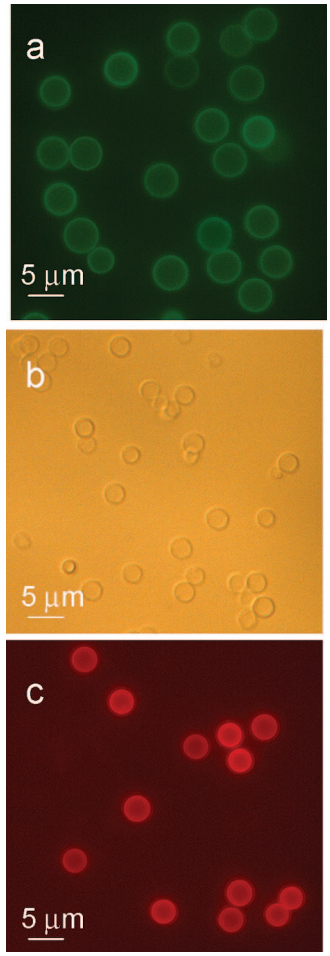

Figure 3. Fluorescence and light microscopy images of 6 μm diameter core−shell silica-PNIPAM-T_{30}/PNIPAM-A_{30} particles stained with PicoGreen (a), (PNIPAM-A_{30}/PNIPAM-T_{30})$_2$/PNIPAM-A_{30} microcapsules after core removal (b), and (PNIPAM-A_{30}/PNIPAM-T_{30})$_2$/PNIPAM-A_{30} microcapsules incubated with rhodamine-labeled PNIPAM micelles (c).

drophobic interactions,[24] this may suggest that both hybridization and hydrophobic interactions are complementary and concomitant driving forces responsible for the growth and stability of the DNA−polymer multilayer films. Both stable and monodisperse microcapsules were formed upon removal of the silica particle template by exposure to pH 5 buffered hydrofluoric acid.[18] Significant capsule shrinkage was observed upon core removal and the diameters decreased to 3.0 ± 0.4 μm (Figure 3b) and 1.0 ± 0.3 μm (Figure 4) from the original core−shell particle sizes of 6 and 3 μm, respectively. Conversely, capsules made solely of diblock DNA do not exhibit such a large shrinkage in diameter.[14−16] The significant shrinkage observed in the DNA−PNIPAM capsules is ascribed to colloidal aggregation and collapse of the hybridized PNIPAM-A_{30} and PNIPAM-T_{30} micelles upon removal of the core. The hydrophobic and more compact domain of PNIPAM in the DNA−PNIPAM nanoparticles contributes to stabilization of the microcapsule shell and is expected to reduce the permeability of the DNA capsule wall (see below). Although the multilayer films were assembled at 500 mM NaCl, the capsules remained intact following post-treatment with lower salt concentrations (200 mM NaCl) (for at least 40 min). As a control experiment, when unmodified PNIPAM micelles were adsorbed on silica, the film immediately disassembled upon dissolution of the silica core, indicating that the DNA sequences are required to drive the assembly of the multilayers and stabilize the final film structure.

DNA−PNIPAM Microcapsule Permeability and Functionalization. The permeability of the shell layer is of crucial consideration when engineering microcapsules, as it determines the access and release of guest molecules to and from the microcapsule core. A comparison between the exclusion properties of hollow PNIPAM-A_{30}/PNIPAM-T_{30} microcapsules and single-component diblock DNA microcapsules toward FITC-labeled dextran (M_w = 70 000 and 500 000 Da) was conducted. Both capsules can be permeated by FITC-dextran of M_w = 70 000 Da (data not shown) but significant differences are observed for capsules incubated with FITC-dextran of M_w = 500 000 Da (Figure 5). Within 30 min of incubation with FITC-dextran of M_w = 500 000, the interior of neat DNA capsules became fluorescent (Figure 5a), as the wall is permeable to the R_h = 15.9 nm macromolecule.[28] In contrast, the interior of the hybrid DNA−PNIPAM microcapsules remained dark (Figure 5b), indicating that the dextran did not permeate through the microcapsule wall after 30 min. The fluorescence intensity profiles across each microcapsule are shown below their corresponding confocal microscopy image in Figure 5. These findings can be explained by a reduced permeability and a more compact structure of the multilayer walls when the microcapsules are composed of DNA−PNIPAM as opposed to DNA alone.

To demonstrate functionality of the capsules, fluorescently labeled, azide-terminated PEG was coupled to the alkyne moieties within the microcapsule shell (Scheme 1b, Figure 6). This occurred within 5 min and only in the presence of Cu(I) which acts as a catalyst, therefore ruling out any nonspecific binding of azides with the microcapsules. Such PEGylation is favorable since it can prevent protein adsorption and thus control DNA hydrolysis from DNase. XPS and FTIR spectros-

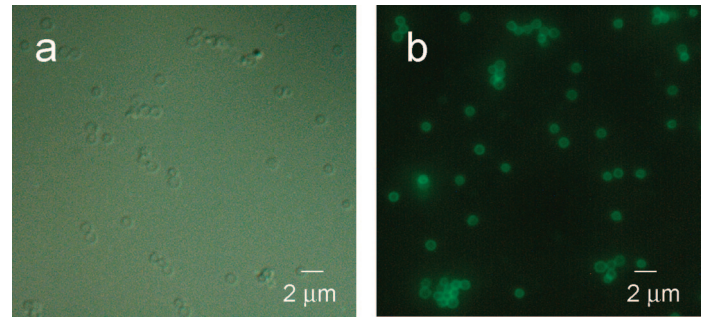

Figure 4. (a) Light and (b) fluorescence microscopy (stained with PicoGreen) images of (PNIPAM-A_{30}/PNIPAM-T_{30})$_2$/PNIPAM-A_{30} microcapsules.

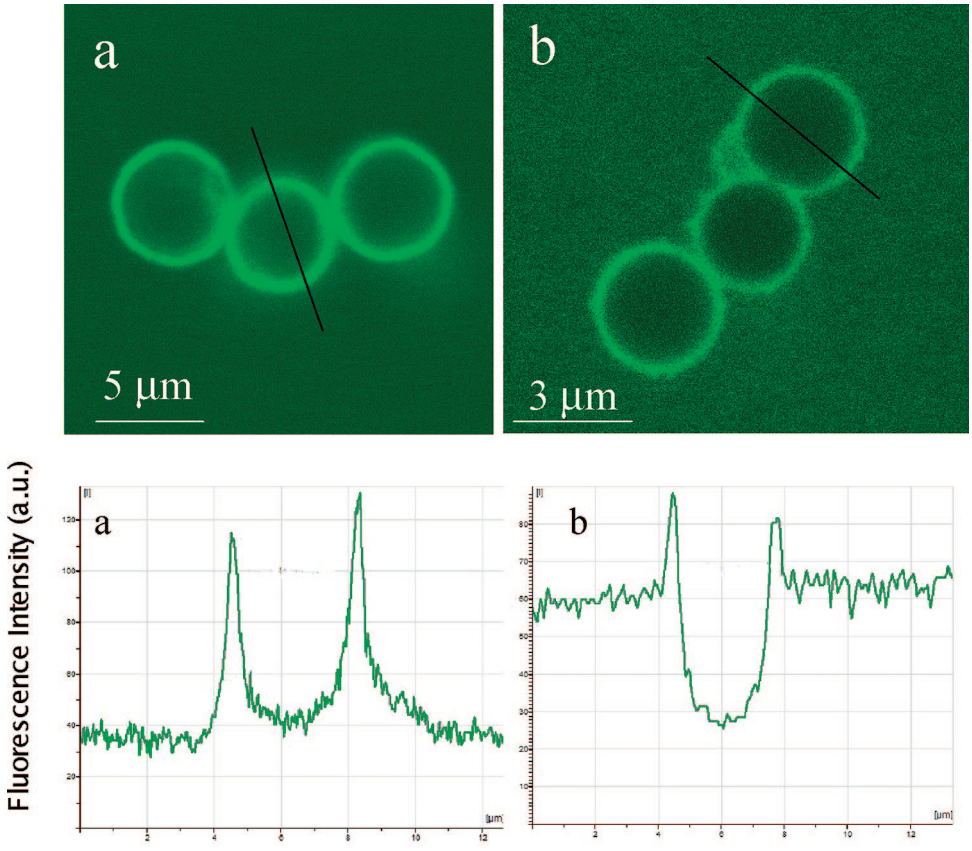

Figure 5. Confocal microscopy images of the permeation of FITC-dextran (M_W 500 000) into five-layer microcapsules of single-component diblock DNA (polyA$_{30}$G$_{30}$/polyT$_{30}$C$_{30}$) (a, top) and PNIPAM-A$_{30}$/PNIPAM-T$_{30}$ (b, top). Corresponding fluorescence intensity profiles along the black line (bottom).

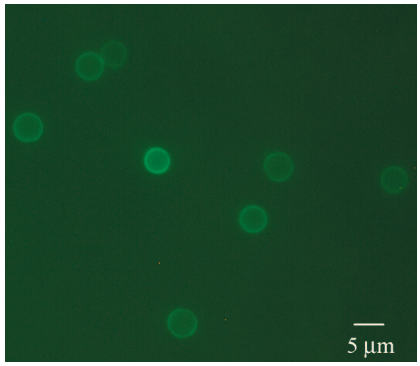

Figure 6. Fluorescence microscopy image of (PNIPAM-A$_{30}$/PNIPAM-T$_{30}$)$_2$/PNIPAM-A$_{30}$ microcapsules incubated with Alexa Fluor 488-labeled azide-terminated PEG.

on the hybridization of complementary oligonucleotide-capped micelles. Films assembled from single homopolymeric oligonucleotides (polyT$_{30}$/polyA$_{30}$) or unmodified PNIPAM micelles resulted in limited film buildup, which disassembled immediately upon dissolution of the silica core. In contrast, PNIPAM-A$_{30}$ and PNIPAM-T$_{30}$ micelles are suitable building blocks for the formation of DNA−polymer thin films and microcapsules. PNIPAM-A$_{30}$ and PNIPAM-T$_{30}$ can be sequentially assembled into multilayer films on both planar and particle substrates. Following removal of the particle core by dissolution, DNA−polymer microcapsules are obtained. In contrast to the single-component diblock DNA microcapsules, the PNIPAM-A$_{30}$/PNIPAM-T$_{30}$ microcapsules were not permeable to FITC-dextran with a M_w of 500 000 Da. The covalent attachment of azide-terminated PEG chains within the core domain of the "click" functionalized PNIPAM micelles demonstrated selective functionalization of the preformed microcapsules.

The design of multilayers combining oligonucleotide building blocks with synthetic organic molecules introduces additional motifs to the DNA assemblies, providing structural and functional advantages that may be exploited for drug delivery applications. For example, the release of therapeutics from such microcapsules can potentially be stimuli-triggered by ionic strength, temperature (as PNIPAM is thermoresponsive), or enzymatic erosion of DNA. The use of PNIPAM-A$_{30}$/PNIPAM-T$_{30}$ capsules for the loading and delivery of anticancer drugs and siRNA is currently under investigation.

In conclusion, we have demonstrated the LbL assembly of hybrid DNA−PNIPAM microcapsules based on the hybridization of complementary oligonucleotide-capped micelles. Films assembled from single homopolymeric oligonucleotides (polyT$_{30}$/polyA$_{30}$) or unmodified PNIPAM micelles resulted in limited film buildup, which disassembled immediately upon dissolution of the silica core. In contrast, PNIPAM-A$_{30}$ and PNIPAM-T$_{30}$ micelles are suitable building blocks for the formation of DNA−polymer thin films and microcapsules. PNIPAM-A$_{30}$ and PNIPAM-T$_{30}$ can be sequentially assembled into multilayer films on both planar and particle substrates. Following removal of the particle core by dissolution, DNA−polymer microcapsules are obtained. In contrast to the single-component diblock DNA microcapsules, the PNIPAM-A$_{30}$/PNIPAM-T$_{30}$ microcapsules were not permeable to FITC-dextran with a M_w of 500 000 Da. The covalent attachment of azide-terminated PEG chains within the core domain of the "click" functionalized PNIPAM micelles demonstrated selective functionalization of the preformed microcapsules.

The design of multilayers combining oligonucleotide building blocks with synthetic organic molecules introduces additional motifs to the DNA assemblies, providing structural and functional advantages that may be exploited for drug delivery applications. For example, the release of therapeutics from such microcapsules can potentially be stimuli-triggered by ionic strength, temperature (as PNIPAM is thermoresponsive), or enzymatic erosion of DNA. The use of PNIPAM-A$_{30}$/PNIPAM-T$_{30}$ capsules for the loading and delivery of anticancer drugs and siRNA is currently under investigation.

copy were used to characterize the film composition before and after PEG functionalization. However, the chemical complexity of the mutilayer film did not allow direct spectroscopic verification of the formation of the 1,2,3 triazole. We are currently investigating "click" chemistry as a versatile approach for loading the microcapsules with therapeutic molecules.

METHODS

Materials. The solvents were AR grade and were used as received. Azobis(isobutyronitrile) (AIBN) was obtained from Sigma-Aldrich and purified by crystallization from methanol. Monomers were purified immediately prior to use. Propargyl acrylate (Sigma-Aldrich) was filtered through neutral alumina (70−230 mesh), *N*-isopropylacrylamide (Sigma-Aldrich) was recrystallized twice from benzene/hexane 3:2 (v:v) and dried under vacuum, and *N*-acryloxysuccinimide (Sigma-Aldrich) was used as received. Sodium chloride, sodium citrate, and 3-aminopropyltrimethoxysilane (APS) were obtained from Sigma-Aldrich. *O*-(2-Aminoethyl)-*O*′-(2-azidoethyl)pentaethylene glycol was purchased from Fluka. 5′-end amine-modified oligonucleotides (NH_2AAAAAAAAAAAAAAAAAAAAAAAAAAAAAA and NH_2TTTTTTTTTTTTTTTTTTTTTTTTTTTTTT) were custom syn-

thesized by Geneworks (Adelaide, Australia). The homopolymeric oligonucleotides polydeoxyadenylic acid and polydeoxythymidilic acid are abbreviated as polyA$_{30}$ and polyT$_{30}$, respectively, and the DNA-grafted polymer systems PNIPAM-A$_{30}$ and PNIPAM-T$_{30}$; 3 and 6 μm diameter silica particles were purchased from MicroParticles (Germany). PicoGreen and Alexa Fluor 488 succinimidyl ester were supplied by Molecular Probes. High-purity water with a resistivity greater than 18 MΩ was obtained from an in-line Millipore RiOs/Origin system (MilliQ water).

Synthesis and Characterization of the PNIPAM Terpolymer. The synthesis of the butyl phthalimidomethyl trithiocarbonate RAFT agent was reproduced on the same scale as described in the literature.[29] The RAFT agent (21.8 mg, 6.7×10^{-5} mol), *N*-isopropylacrylamide (1 g, 8.8×10^{-3} mol), propargyl acrylate (54 mg, 4.9×10^{-4} mol), *N*-acryloxysuccinimide (76 mg, 4.5×10^{-4} mol), and AIBN (1.65 mg, 1.0×10^{-5} mol) were combined in 5 mL of dioxane in a Schlenk flask. The flask was purged with nitrogen, degassed by four freeze−evacuate−thaw cycles, sealed under vacuum, and then heated in a constant temperature oil bath at 60 °C for 16 h. The polymerization was quenched by placing the flask in liquid nitrogen and a sample of the monomer/polymer mixture was diluted with $CDCl_3$ for NMR analysis. The final yellowish product was isolated by precipitation from dioxane into hexane, followed by filtration and drying (×2). ^{1}H NMR (Bruker 300 MHz) ($CDCl_3$) (polymer) ppm: 0.9−1.1 CH_3 (polymer), 1.0−2.2 CH_2 (polymer), 2.45 CH−C═O (polymer), 2.9 (*N*-hydroxysuccinimide protons), 4.0 CH−N (polymer), 4.85 CH_2 (propargyl group), 7.8 (aromatic phthalimido protons). $Mn_{(NMR)}$ = 16 000 g mol^{-1}; monomer conversion determined by NMR = 95%.

Conjugation of Oligonucleotides to the PNIPAM Terpolymer. In a typical preparation, 5 μM of 5′-end amine-polyT$_{30}$ and 5′-end amine-polyA$_{30}$ were incubated with the PNIPAM random terpolymer in an aqueous solution at a concentration higher than the critical aggregation concentration (cac) (2 mg mL^{-1}) to yield DNA-decorated micelles. The reaction mixture was incubated at 20 °C for 4 days and dialyzed (cutoff 12 000) against deionized water for the removal of unreacted oligonucleotide. The concentration of DNA was determined by measuring the absorbance at 260 nm using an extinction coefficient of 243 600 and 363 400 M^{-1} cm^{-1} (Agilent 8453 UV−vis) for the amine polyT$_{30}$ and the amine polyA$_{30}$, respectively. The background absorbance of the PNIPAM terpolymer was subtracted from the total absorbance.

Measurement of Critical Aggregation Concentration. To determine the critical aggregation concentration, PNIPAM-*co*-PA-*co*-NAS micelles were typically prepared using the following procedure. The amphiphilic terpolymer was dissolved in a good solvent, DMSO, at a concentration of 1% w/v and the aqueous miscible solvent was gradually replaced by water during dialysis. Final concentrations of dialyzed samples were typically in the range 1−2 mg mL^{-1}. The aggregation behavior of the random terpolymer was studied using pyrene as a fluorescent probe. Sample solutions were prepared according to the method used by Eisenberg and co-workers[30] at final concentrations ranging from 0.05−1.15 mg mL^{-1}. Steady-state fluorescence spectra were recorded using a Flurolog Horiba fluorescence spectrophotometer in a 1 cm quartz cell. Fluorescence spectra were acquired at 23 °C using an excitation wavelength of 339 nm with a slit width of 2 nm. Dynamic light scattering (DLS) analysis was performed on a Malvern Zetasizer equipped with a single angle backscatter system and a temperature controller. Samples were filtered through a 0.25 μm filter and equilibrated to 23 °C prior to measurement.

Quartz Crystal Microgravimetry. QCM measurements were made using a Q-Sense E4 instrument equipped with a flow cell (Q-Sense AB, Västra Frölunda, Sweden). The QCM mass sensitivity factor is 17.7 ng cm^{-2} Hz^{-1}. The temperature was fixed at 23 °C during the experiments. A gold-coated 5 MHz AT-cut crystal with a fundamental resonant frequency of about 5 MHz was used, operating both in frequency and dissipation at its third harmonic. Gold-coated crystals were cleaned with Piranha solution (70/30 v/v % sulfuric acid:hydrogen peroxide). *Caution! Piranha solution is highly corrosive and oxidative. Extreme care should be taken when handling Piranha solution and only small aliquots should be prepared.* Large dissipation changes observed in the experiments invalidated the linear relationship (Sauerbrey equation) between the deposited mass and frequency shift. Hence the QCM data for the assembly of the multilayer films are quoted as frequency shifts rather than absolute mass changes. After initially depositing a layer of polyT$_{30}$ (5 μM for 15 min), PNIPAM-A$_{30}$ micelle and PNIPAM-T$_{30}$ micelle (230 μL of 1 μM oligonucleotide and 0.6 mg mL^{-1} PNIPAM micelles in SSC buffer) adsorption was recorded for 2 h. After each adsorption step, the film was washed with 1 mL of SSC buffer (0.5 M NaCl, pH 6.5).

Multilayer Formation on Particles and Capsule Formation. To surface-functionalize the silica particles with amines, a suspension of 3- (or 6-) μm diameter SiO_2 particles in 1 mL of ethanol was reacted with 250 μL of APS and 50 μL of 25 v/v % ammonia solution, overnight. The particles were washed twice with ethanol and three times with Milli-Q water. After initially depositing a layer of polyT$_{30}$ (5 μM for 15 min), the PNIPAM-A$_{30}$ and PNIPAM-T$_{30}$ multilayers were deposited on the amine-functionalized particles by incubating 20 μL of the particles in 100 μL of PNIPAM-A$_{30}$ and PNIPAM-T$_{30}$ (of 1 μM oligonucleotide and 0.6 mg mL^{-1} PNIPAM micelles in SSC buffer) for 2 h. After adsorption, the particles were washed three times in SSC buffer before the addition of the next layer. The silica core was dissolved within a few minutes by mixing 1 μL of the particle suspension with 10 μL of ammonium fluoride (0.4)/hydrofluoric acid (0.25 M) buffered at pH 5. The coated microparticles and microcapsules were imaged on an Olympus IX71 digital wide-field fluorescence microscope equipped with a fluorescein isothiocyanate (FITC) and tetramethyl rhodamine isocyanate (TRITC) filter cube, a differential interference contrast (DIC) slider (U-DICT, Olympus), and 60× objective lens. A CCD Camera (Cool SNAP fx, Photometrics, Tucson, AZ) was mounted on the left-hand port of the microscope. Microcapsules prepared following the above procedure were incubated in 0.3 mg mL^{-1} of M_W 70 000 and M_W 500 000 FITC-dextran for 30 min in SSC buffer (0.5 M NaCl, pH 6.5) at room temperature. Different acquistion gains were used for the two permeability experiments in order to optimize the fluorescence profile. The melting curves for the DNA multilayers were determined by suspending 2×10^6 particles mL^{-1} in SSC buffer in the presence of 0.06 μM PicoGreen and monitoring the fluorescence emission of PicoGreen at 520 nm (excitation wavelength = 480 nm) over a range of temperatures. Confocal microscopy experiments were performed on a Leica TCS-SP2 confocal scanning microscope using an excitation wavelength of 488 nm. Azide PEG amine was labeled by using Alexa Fluor 488 succinimidyl ester in water for 2 h and was purified using a Sephadex column. Fifty microliters of the microparticle suspension (50 mg mL^{-1}) was incubated for 10 min with 0.5 mg mL^{-1} of the fluorescently labeled azide PEG in the presence of copper sulfate (20 μL, 1.8 mg mL^{-1}) and sodium ascorbate (20 μL, 4.4 mg mL^{-1}) for 5 min and the particles were subsequently washed three times in SSC buffer.

Acknowledgment. This work was supported by funding from the ARC under the Linkage International, Discovery Project and Federation Fellowship Schemes.

Supporting Information Available: The structure of the PNIPAM random terpolymer (PNIPAM-*co*-PA-*co*-NAS); the emission spectra of pyrene in an aqueous solution of the PNIPAM random copolymer; size distributions of PNIPAM terpolymer micelles and PNIPAM-A$_{30}$ and PNIPAM-T$_{30}$; the melting curve for the hybridized strands within the multilayer assembly of PNIPAM-A$_{30}$ and PNIPAM-T$_{30}$. This material is available free of charge *via* the Internet at http://pubs.acs.org.

REFERENCES AND NOTES

1. Gibbs, J. M.; Park, S.-J.; Anderson, D. R.; Watson, K. J.; Mirkin, C. A.; Nguyen, S. T. Polymer- DNA Hybrids as Electrochemical Probes for the Detection of DNA. *J. Am. Chem. Soc.* **2005**, *127*, 1170–1178.
2. Miyamoto, D.; Tang, Z.; Takarada, T.; Maeda, M. Turbidimetric Detection of ATP Using Polymeric Micelles and DNA Aptamers. *Chem. Commun.* **2007**, *45*, 4743–4745.
3. Tang, Z.; Takarada, T.; Sato, Y.; Maeda, M. Colloidal Nanoparticles from Poly(*N*-isopropylacrylamide)-*graft*-DNA for Single Nucleotide Discrimination Based on Salt-

Induced Aggregation: Extension to Long Target DNA. *Chem. Lett.* **2004**, *33*, 1602–1603.
4. Alemdaroglu, F. E.; Ding, K.; Berger, R.; Herrmann, A. DNA-Templated Synthesis in Three Dimensions: Introducing a Micellar Scaffold for Organic Reactions. *Angew. Chem., Int. Ed.* **2006**, *45*, 4206–4210.
5. Mori, T.; Umeno, D.; Maeda, M. Sequence-Specific Affinity Precipitation of Oligonucleotide using Poly(*N*-isopropylacrylamide)-Oligonucleotide Conjugate. *Biotechnol. Bioeng.* **2001**, *72*, 261–268.
6. Costioli, M. D.; Fisch, I.; Garret-Flaudy, F.; Hilbrig, F.; Freitag, R. DNA Purification by Triple-Helix Affinity Precipitation. *Biotechnol. Bioeng.* **2003**, *81*, 535–545.
7. Jeong, J. H.; Park, T. G. Novel Polymer-DNA Hybrid Polymeric Micelles Composed of Hydrophobic Poly(D, L-lactic-*co*-glycolic Acid) and Hydrophilic Oligonucleotides. *Bioconjugate Chem.* **2001**, *12*, 917–923.
8. Li, Z.; Zhang, Y.; Fullhart, P.; Mirkin, C. A. Reversible and Chemically Programmable Micelle Assembly with DNA Block-Copolymer Amphiphiles. *Nano Lett.* **2004**, *4*, 1055–1058.
9. Ding, K.; Alemdaroglu, F. E.; Börsch, M.; Berger, R.; Herrmann, A. Engineering the Structural Properties of DNA Block Copolymer Micelles by Molecular Recognition. *Angew. Chem., Int. Ed.* **2007**, *46*, 1172–1175.
10. Alemdaroglu, F. E.; Herrmann, A. DNA Meets Synthetic Polymers—Highly Versatile Hybrid Materials. *Org. Biomol. Chem.* **2007**, *5*, 1311–1320.
11. Alemdaroglu, F. E.; Wang, J.; Börsch, M.; Berger, R.; Herrmann, A. Enzymatic Control of the Size of DNA Block Copolymer Nanoparticles. *Angew. Chem., Int. Ed.* **2008**, *47*, 974–976.
12. Alemdaroglu, F. E.; Alemdaroglu, N. C.; Langguth, P.; Herrmann, A. Cellular Uptake of DNA Block Copolymer Micelles with Different Shapes. *Macromol. Rapid Commun.* **2008**, *29*, 326–329.
13. Alemdaroglu, F. E.; Alemdaroglu, N. C.; Langguth, P.; Herrmann, A. DNA Block Copolymer Micelles—A Combinatorial Tool for Cancer Nanotechnology. *Adv. Mater.* **2008**, *20*, 899–902.
14. Johnston, A. P. R.; Read, E. S.; Caruso, F. DNA Multilayer Films on Planar and Colloidal Supports: Sequential Assembly of Like-Charged Polyelectrolytes. *Nano Lett.* **2005**, *5*, 953–956.
15. Johnston, A. P. R.; Mitomo, H.; Read, E. S.; Caruso, F. Compositional and Structural Engineering of DNA Multilayer Films. *Langmuir* **2006**, *22*, 3251–3258.
16. Johnston, A. P. R.; Caruso, F. Exploiting the Directionality of DNA: Controlled Shrinkage of Engineered Oligonucleotide Capsules. *Angew. Chem., Int. Ed.* **2007**, *46*, 2677–2680.
17. Kataoka, K.; Harada, A.; Nagasaki, Y. Block Copolymer Micelles for Drug Delivery: Design, Characterization and Biological Significance. *Adv. Drug Deliv. Rev.* **2001**, *47*, 113–131.
18. Zelikin, A. N.; Becker, A. L.; Johnston, A. P. R.; Wark, K. L.; Turatti, F.; Caruso, F. A General Approach for DNA Encapsulation in Degradable Polymer Microcapsules. *ACS Nano* **2007**, *1*, 63–69.
19. Oster, C. G.; Kim, N.; Grode, L.; Barbu-Tudoran, L.; Schaper, A. K.; Kaufmann, S. H. E.; Kissel, T. Cationic Microparticles Consisting of Poly(lactide-co-glycolide) and Polyethylenimine as Carriers Systems for Parental DNA Vaccination. *J. Controlled Release* **2005**, *104*, 359–377.
20. Moad, G.; Rizzardo, E.; Thang, S. H. Living Radical Polymerization by the RAFT Process. *Aust. J. Chem.* **2005**, *58*, 379–410.
21. Moad, G.; Li, G.; Postma, A.; Rizzardo, E.; Thang, S. H.; Pfaendner, R.; Wermter, H. RAFT Copolymerization and Its Application to the Synthesis of Novel Dispersants-Intercalants-Exfoliants for Polymer-Clay Nanocomposites: Some Interesting Results from RAFT Copolymerization. *ACS Symp. Ser.* **2006**, *944*, 514–532.
22. Rostovtstev, V. V.; Green, L. G.; Fokin, V. V.; Sharpless, K. B. H. A Stepwise Huisgen Cycloaddition Process: Copper(I)-Catalyzed Regioselective "Ligation" of Azides and Terminal Alkynes. *Angew. Chem., Int. Ed.* **2002**, *41*, 2596–2599.
23. Cavalieri, F.; Chiessi, E.; Paradossi, G. Chaperone-Like Activity of Nanoparticles of Hydrophobized Poly(vinyl alcohol). *Soft Matter* **2007**, *3*, 718–724.
24. Kujawa, P.; Watanabe, H.; Tanaka, F.; Winnik, F. M. Amphiphilic Telechelic Poly(*N*-isopropylacrylamide) in Water: From Micelles to Gels. *Eur. Phys. J. E* **2005**, *17*, 129–137.
25. Schweitzer, C.; Scaiano, J. C. Selective Binding and Local Photophysics of the Fluorescent Cyanine Dye PicoGreen in Double-Stranded and Single-Stranded DNA. *Phys. Chem. Chem. Phys.* **2003**, *5*, 4911–4917.
26. Ishida, N.; Biggs, S. Salt-Induced Structural Behavior for Poly(*N*-isopropylacryamide) Grafted onto Solid Surface Observed Directly by AFM and QCM-D. *Macromolecules* **2007**, *40*, 9045–9052.
27. Liu, G.; Cheng, H.; Yan, L.; Zhang, G. Study of the Kinetics of the Pancake-to-Brush Transition of Poly(*N*-isopropylacrylamide) Chains. *J. Phys. Chem. B* **2005**, *109*, 22603–22607.
28. Armstrong, J. K.; Wenby, R. B.; Meiselman, H. J.; Fisher, T. C. The Hydrodynamic Radii of Macromolecules and Their Effect on Red Blood Cell Aggregation. *Biophys. J.* **2004**, *87*, 4259–4270.
29. Postma, A.; Davis, T. P.; Evans, R. A.; Li, G.; Moad, G.; O'Shea, M. S. Synthesis of Well-Defined Polystyrene with Primary Amine End Groups through the Use of Phthalimido-Functional RAFT Agents. *Macromolecules* **2006**, *39*, 5293–5306.
30. Astafieva, I.; Zhong, X. F.; Eisenberg, A. Critical Micellization Phenomena in Block Polyelectrolyte Solutions. *Macromolecules* **1993**, *26*, 7339–7352.